Chinese Science Bulletin

An electrochemical impedance spectroscopic study of the electronic and ionic transport properties of $LiCoO_2$ cathode

ZHUANG QuanChao[1,3], XU JinMei[1], FAN XiaoYong[1], DONG QuanFeng[1,2], JIANG YanXia[1], HUANG Ling[1] & SUN ShiGang[1†]

[1] State Key Laboratory of Physical Chemistry of Solid Surfaces, Department of Chemistry, College of Chemistry and Chemical Engineering, Xiamen University, Xiamen 361005, China;
[2] Power-long Battery Research Institute, Xiamen University, Xiamen 361005, China;
[3] Northwest Institute of Nuclear Technology, Xi'an 710024, China

The storage behavior and process of the first delithiation-lithiation of $LiCoO_2$ cathode were investigated by electrochemical impedance spectroscopy (EIS). The electronic and ionic transport properties of $LiCoO_2$ cathode along with variation of electrode potential were obtained in 1 mol·L^{-1} $LiPF_6$-EC:DMC:DEC electrolyte solution. It was found that after 9 h storage of the $LiCoO_2$ cathode in electrolyte solutions, a new arc appears in the medium frequency range in Nyquist plots of EIS, which increases with increasing the storage time. In the charge/discharge processes, the diameter of the new arc is reversibly changed with electrode potential. Such variation coincides well with the electrode potential dependence of electronic conductivity of the $LiCoO_2$. Thus this new EIS feature is attributed to the change of electronic conductivity of Li_xCoO_2 during storage of the $LiCoO_2$ cathode in electrolyte solutions, as well as in processes of intercalation-deintercalationtion of lithium ions. It has been revealed that the reversible increase and decrease of the resistance of SEI film in charge-discharge processes can be also ascribed to the variation of electronic conductance of active materials of the $LiCoO_2$ cathode.

Li-ion batteries, $LiCoO_2$, EIS, SEI film, electronic conductivity

$LiCoO_2$ is the most widely used cathode material today in commercially available Li-ion batteries, due to its high energy density, low self-discharge and good cycle life performance[1−3]. In the past decade, the $LiCoO_2$ and, in general, its derivatives $Li_xNi_{1-y}Co_yO_2$ have been studied extensively as cathode materials for Li-ion batteries. However, the electronic conductivity, electronic structure, and phase transitions of these cathode materials as well as the effect of these properties on electrochemical performance need to be investigated in detail[4−7]. The literature data[2,8−10] leave no doubts about the existence of a drastic change of the electronic conductivity occurring at early stage of lithium deintercalation, which may be caused by a transition from insulator to metal (or so called metal-insulator transition). In case of Li_xCoO_2 materials, such transition has been proposed to be responsible for the existence of a two-phase region between the lithium concentrations of $x = 0.95$ and $x = 0.75$, namely, Li_xCoO_2 is a semiconductor for $x > 0.95$, and is of metallic property for $x < 0.75$.

Electrochemical impedance spectroscopy (EIS), is one of the most powerful means to analyze electrochemical processes occurring at electrode/electrolyte interfaces, and has been widely applied to the studies of electrochemical lithium intercalation into carbonaceous materials and transition metal oxides. The Nyquist plots

Received September 7, 2006; accepted December 28, 2006
doi: 10.1007/s11434-007-0169-1
†Corresponding author (email: sgsun@xmu.edu.cn)
Supported by the Special Funds for Major State Basic Research Project of China (Grant No. 2002CB211804)

of electrochemical lithium intercalation into $LiCoO_2$-based electrodes commonly consist of three parts, namely, the first arc in the high-frequency range (HFA), the second arc in the medium frequency (MFA) range, and an incline line in the low frequency range. The HFA is generally attributed to the migration of lithium ions through a surface film (also called solid electrolyte interphase (SEI)) on $LiCoO_2$, the MFA is ascribed to the charge transfer step, and the incline line in the low frequency range reflects the solid state diffusion process of lithium ions into $LiCoO_2$ that is often described as finite space or restricted diffusion[11−15]. However, Croce and coworkers[16−21] considered that the drastic change in resistance caused by the insulator to metal transition must be necessarily reflected by the impedance dispersion, namely, the Nyquist plots of $LiCoO_2$ in the delithiated state should involve a third arc relating to the electronic properties of the material. Therefore, the Nyquist plots of electrochemical lithium intercalation into $LiCoO_2$-based electrode should include four parts, i.e. the first arc in the high-frequency range (HFA), the second arc in the medium-frequency range (MFA), the third arc in the low-frequency range (LFA), and an incline line in the very low frequency range. They proposed that the HFA is related to the migration of lithium ions through SEI film on the $LiCoO_2$ electrode, the MFA is attributed to the charge transfer step, the LFA is associated with the electronic properties of the material, and the incline line in the very low frequency range reflects the ionic diffusion. The experimental results of Croce et al. were nevertheless analogous to those previously reported by other authors, and from their Nyquist plots, the three obviously separated semicircles could not be observed. Moreover, the Nyquist plots of electrodes of the $LiCoO_2$ and its derivative materials $Li_xNi_{1-y}Co_yO_2$, which they obtained at low potentials (below 3.7 V), were also analogous to previously reported results consisting of two parts: 1) an arc in the high-frequency range relating to migration of lithium ions through the SEI film, and 2) a sloping line in the low-frequency range that is generally attributed to the charge transfer process or the blocking characteristic of the electrode. Croce and coworkers[16−21] attributed nevertheless the sloping line in low-frequency range to the electronic properties of the material. It is well known that the practical $LiCoO_2$ cathodes are composite materials, in which the active mass particles are bound to an aluminum current collector with a polymeric binder such as polyvinylidene difuoride (PVdF). In addition, the composite electrodes have to contain a conductive additive, usually carbon particles (e.g. carbon black, graphite). The electrodes are usually prepared from slurry of the particles and the binder in an organic solvent, which is spread on the current collector, followed by drying. The final shape of the electrode is obtained by applying some pressure to the electrode. So, its electronic conductivity must be affected by the amount of conductive additive in the $LiCoO_2$ composite materials and by the contact between the $LiCoO_2$ cathode film and the aluminum current collector. As a consequence, variation of electronic conductivity of the active mass with electrode potential change can be observed only when the $LiCoO_2$ cathode contains enough amount of conductive additive, and has a good contact between the $LiCoO_2$ cathode film and the aluminum current collector. In addition, when the $LiCoO_2$ cathode contacts non-aqueous organic electrolytes, spontaneous reactions may take place at surface of the cathode and form a thick surface film on it. Along with the dissolution of lithium ions from $LiCoO_2$ electrochemical inactive Co_3O_4 may be formed[22−24]. It can be deduced that the electronic conductivity of the $LiCoO_2$ cathode may be greatly affected by the above processes. Based on the above analysis, the $LiCoO_2$ cathode containing high weight percent of conductive additive and PVdF binder (10 wt%) was prepared in this study, and the $LiCoO_2$ cathode after drying was compressed by a rolling machine (between iron wheels) in order to obtain a good contact between the $LiCoO_2$ cathode film and the aluminum current collector. The storage behavior and process of first delithiation-lithiation of the $LiCoO_2$ cathode were investigated by EIS. The electronic and ionic transport properties of the $LiCoO_2$ cathode were obtained for the storage and the process of the first delithiation-lithiation in 1 $mol \cdot L^{-1}$ $LiPF_6$-EC:DMC:DEC electrolyte solutions.

1 Experiment

All experiments were carried out in a three-electrode glass cell with Li foils as both auxiliary and reference electrodes. The $LiCoO_2$ cathode composition was 80 weight percent (wt%) $LiCoO_2$ powder (B&M Ltd Co., Tianjin, China), 10 wt% ploy vinylidene fluoride binder (Kynar FLEX 2801, Elf-atochem, USA), 3 wt% carbon black and 7 wt% graphite (Shanshan limited Co.

Shanghai, China), and an aluminum foil was used as current collector. The electrolyte was 1 mol·L^{-1} $LiPF_6$-EC:DMC:DEC (volume ratio 1:1:1, Guotaihuarong Co., Zhangjiagang, China).

EIS measurements were carried out in an electrochemical work station (CHI660b, Chenhua Ltd Co., Shanghai, China). The amplitude of ac perturbation signal was 5 mV and the frequency range was from 10^5 to 10^{-2} Hz. The electrode was equilibrated for 1 h before EIS measurements. The impedance data were analyzed using Zview software.

2 Results and discussion

2.1 The common EIS features of $LiCoO_2$ cathode in the storage and in the first charge-discharge process

The Nyquist plots (Figure 1(a)) for the storage of $LiCoO_2$ cathode for 3 and 6 h in electrolyte solutions at open circuit potential, i.e. 3.5 V, display an arc in the high-frequency (HF) range and a slightly inclined line in the low-frequency (LF) region, similar to the results reported in refs. [11−21]. As previously described, the arc in the high-frequency range is related to the migration of lithium ions through SEI film, and the sloping line in the low-frequency range is generally attributed to the charge transfer process or the blocking characteristic of the electrode[11−15]. However, Croce and coworkers attributed the sloping line in the low-frequency range to electronic properties of the material[16−21].

It is found that after 9 h storage of the $LiCoO_2$ cathode in electrolyte solutions, a new arc appears in the medium frequency range (MFA) in Nyquist plots. This new arc increases with the increase of the storage time, but the EIS features remain unchanged till 42 h of storage (Figure 1(b)). The above unique phenomenon has not been reported so far in the literature to our knowledge. Because the electrode potential was set at 3.5 V in the storage of $LiCoO_2$ cathode in electrolyte solutions, the appearance of the new arc must associate with the interaction between $LiCoO_2$ cathode and electrolyte solution species. This corresponds to our previous analysis that in the storage of $LiCoO_2$ cathode in electrolyte solution, spontaneous reactions may take place at surface of the cathode resulting in a thick surface film, and the dissolution of lithium ions from $LiCoO_2$ leads to the formation of electrochemically inactive Co_3O_4. The above processes give rise to change of the electronic conductivity of $LiCoO_2$. Obviously, if the new arc is attributed to charge transfer step according to Croce et al., the above phenomenon could not be explained properly. Thus the new arc appearing in the medium frequency range in the Nyquist plots after 9 h storage of $LiCoO_2$ cathode in electrolyte solutions should be assigned to electronic properties of the material, and the HFA, MFA, LFA appearing in the Nyquist plots in Figure 1(b) may be attributed to the migration of lithium ions through the SEI films, the electronic properties of the material and the charge transfer step, respectively.

Variations of impedance spectra of $LiCoO_2$ cathode after 42 h storage in electrolyte solution with increase of polarization potential (charge process) are shown in Figure 2. It can be seen that along with increase of electrode potential, the EIS features of $LiCoO_2$ cathode below 3.85 V in the charge process are analogous to those obtained after 9 h storage in electrolyte solution. On charging from 3.85 to 3.9 V, the diameter of the MFA

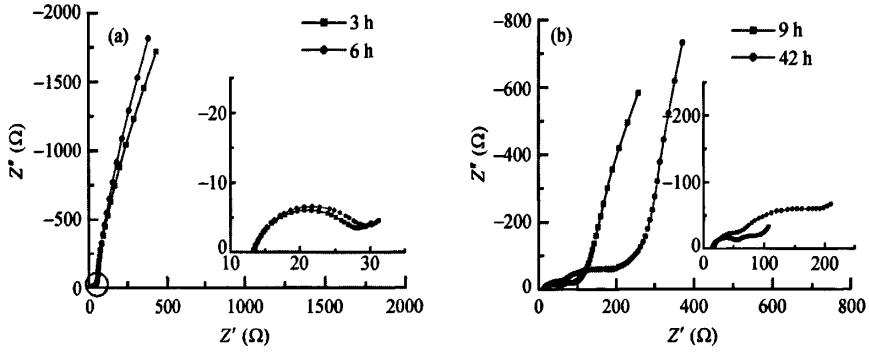

Figure 1 Variations of impedance spectra of $LiCoO_2$ cathode with the increase of the storage time in frequency range 10^5-10^{-2} Hz. The insets in (a) and (b) show the enlarged spectra over a 10^5-50 Hz and $10^5-0.5$ Hz frequency range respectively.

PHYSICAL CHEMISTRY

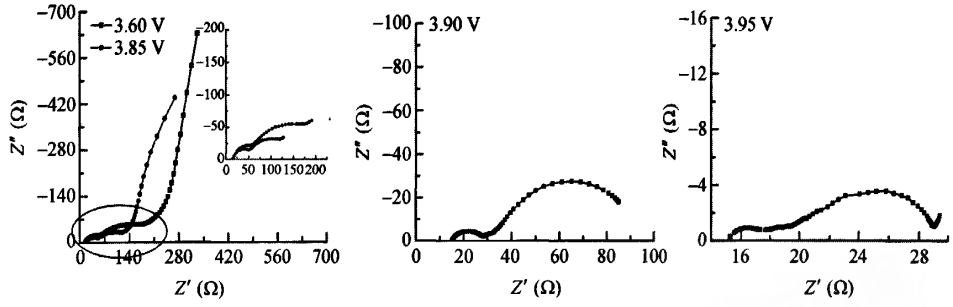

Figure 2 Variations of impedance spectra of $LiCoO_2$ cathode after 42 h storage in the electrolyte solution with the polarization potential in the first charge process in frequency range 10^5-10^{-2} Hz. The inset shows the enlarged spectra over a $10^5-0.5$ Hz frequency range.

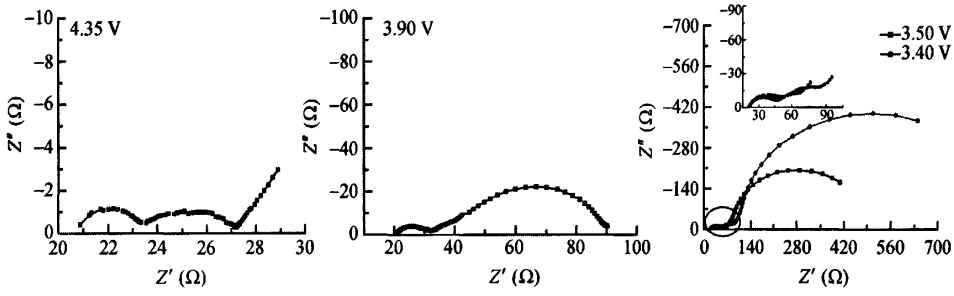

Figure 3 Variations of impedance spectra of $LiCoO_2$ cathode with the polarization potential in the first discharge process in frequency range 10^5-10^{-2} Hz. The inset shows the enlarged spectra over a 10^5-1 Hz frequency range.

decreases rapidly. We could not observe clearly a semicircle in the medium frequency range, the MFA is converted into a sloping line due to the large diameter of the HFA, and the inclined line related to charge transfer step in the low frequency range is bended toward the real axis forming a semicircle. At 3.95 V, a straight line reflecting the solid state diffusion of lithium ions into $LiCoO_2$ appears in the very low frequency range in the Nyquist plots. Thus the spectrum at 3.95 V yields an HFA related to SEI film, a second arc in the medium-frequency region associated with electronic conductivity of the $LiCoO_2$, and a third arc in the low-frequency range corresponding to charge transfer resistance coupled with double layer capacitance, followed by a straight line reflecting solid state Li-ion diffusion in the bulk of active mass in the very low frequency range. On further charging to 4.35 V, the EIS features of $LiCoO_2$ cathode remain analogous to those at 3.95 V in the charge process.

Figure 3 shows variations of impedance spectra of $LiCoO_2$ cathode with the decrease of electrode potential (discharge process). In the experiment, the electrode potential was first swept linearly to 4.35 V at 20 μV/s, and then impedance spectra were recorded along with the decrease of electrode potential. We could not observe three well-separated semicircles at 4.35 V in Nyquist plots due to overlapping of the HFA and the MFA when their diameters are too small. With the decrease of electrode potential, the EIS features of the $LiCoO_2$ cathode above 3.95 V are similar to those at 4.35 V; the EIS features of the $LiCoO_2$ cathode at 3.9 V in discharge process are analogous to those observed at 3.9 V in charge process; a sloping line appears in the medium frequency range and the straight line in the very low frequency range disappears. On further discharging to 3.4 V, the sloping line is converted to a semicircle, while the LFA is translated to a sloping line.

2.2 Equivalent circuit proposed in EIS analysis

According to experimental results obtained in this work, an equivalent circuit, as shown in Figure 4, is proposed to fit the impedance spectra in the storage and the first charge-discharge process. In this equivalent circuit, R_s represents the ohmic resistance; R_{SEI} and R_{ct} are resistances of the SEI film and the charge transfer reaction;

the capacitance of the SEI film, the capacitance of the double layer and the Warburg impedance are represented by the constant phase elements (CPE) Q_{SEI}, Q_{dl} and Q_D, respectively; the electronic resistance of the material and the associated capacitance used to characterize the electronic properties of the material are represented by R_e and the constant phase elements Q_e. The expression for the admittance response of the CPE (Q) is

$$Y=Y_0\omega^n\cos\left(\frac{n\pi}{2}\right)+jY_0\omega^n\sin\left(\frac{n\pi}{2}\right), \quad (1)$$

where ω is the angular frequency, j the imaginary unit. A CPE represents a resistor when $n = 0$, a capacitor with capacitance of C when $n = 1$, an inductor when $n = -1$, and a Warburg resistance when $n = 0.5$. In this study, Y_0 is considered to be a pseudo capacitance (pseudo-Y_0) when n lies between 0.5 and 1.

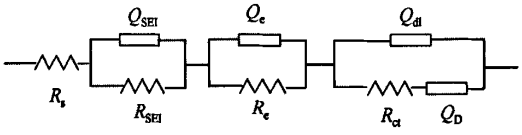

Figure 4 Equivalent circuit proposed for analysis of impedance spectra of $LiCoO_2$ cathode in the storage in electrolyte and the first charge-discharge process.

The simulated impedance spectra are compared with experimental EIS data at 3.5 V in the discharge process in Figure 5, and the parameter values are listed in Table 1. It can be seen that the proposed model can satisfactorily describe the experimental data. The relative standard deviation for all parameters fitted does not exceed 15%.

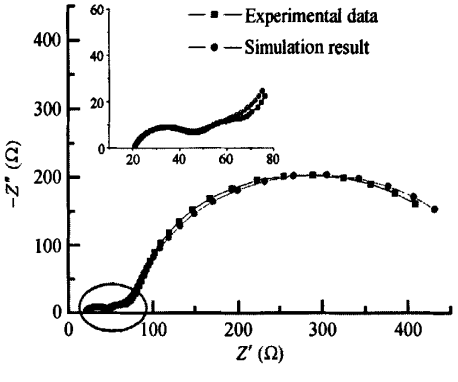

Figure 5 Comparison of EIS experimental data at 3.5 V in the discharge process with simulation results using equivalent circuit of Figure 4.

2.3 Storage behavior of the $LiCoO_2$ cathode in electrolyte solutions

Figure 6 shows variations of EIS parameters obtained from fitting the experimental impedance spectra of the $LiCoO_2$ cathode with increasing the storage time at open circuit potential. It can be seen that with the increase of storage time, R_{SEI} and Q_{SEI}-n keep invariable, while Q_{SEI}-Y_0 continuously increases till 30 h storage, and keeps invariable after 30 h storage. These results indicate that a highly passivating SEI film has been formed on surface of the $LiCoO_2$ cathode after 9 h storage, thus the aging process of the SEI film dominates the electrode surface chemistry between 9 and 30 h. It is well known that the electrolyte solutions may be unavoidably contaminated by trace water, and in the aging process of the SEI film H_2O may react with components of the SEI film such as organic carbonate lithium compounds $ROCO_2Li$ to yield Li_2CO_3, leading to the dissolution of part of organic components of the SEI film and to the increase of capacitance of the SEI film.

Table 1 Equivalent circuit parameters obtained from simulation of EIS experimental data at 3.5 V in the discharge process

Parameter	Value	Uncertainty
R_s (Ω)	20.75	0.70549%
R_{SEI} (Ω)	24.47	4.085%
Q_{SEI}-Y_0(F)	3.4614×10^{-5}	15.903%
Q_{SEI}-n	0.77337	2.2416%
R_e (Ω)	29.66	7.6092%
Q_e-Y_0(F)	0.002062	13.736%
Q_e-n	0.69975	5.9917%
R_{ct} (Ω)	465.2	1.775%
Q_{dl}-Y_0(F)	0.0084102	1.3786%
Q_{dl}-n	0.91124	0.94703%
χ^2=0.0012681		

With the increase of storage time, R_e increases, Q_e-n keeps invariable, while Q_e-Y_0 decreases, implying that the electronic conductivity of the material is strongly affected by the storage time of the $LiCoO_2$ cathode in electrolyte solutions. Because the electrode potential is always maintained at 3.5 V during storage of the $LiCoO_2$ cathode in electrolyte solution, we may conclude that the electronic conductivity is affected not solely by the electrode potential, but the storage time of the $LiCoO_2$ cathode in electrolyte solutions plays a major role. Wang et al. reported that the storage of $LiCoO_2$ in electrolyte solutions may lead to the dissolution of lithium ions from $LiCoO_2$ and the formation of electrochemically inactive Co_3O_4 compound. Therefore the variation of electronic

conductivity in storage of the $LiCoO_2$ cathode in electrolyte solutions may be ascribed to the degradation in structure of the $LiCoO_2$.

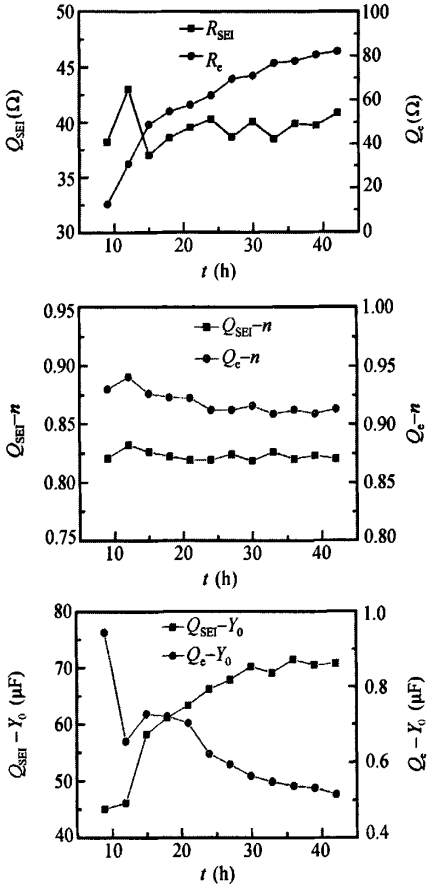

Figure 6 Variations of EIS parameters obtained from fitting the experimental impedance spectra of the $LiCoO_2$ cathode with the increase of storage time at open circuit potential (OCP, 3.5 V).

2.4 EIS studies of the $LiCoO_2$ cathode in the first charge-discharge process

Variations of R_{SEI} and R_e with increase and decrease of electrode potential obtained from fitting the experimental impedance spectra of the $LiCoO_2$ cathode in the first charge-discharge process are shown in Figures 7 and 8, respectively. It can be observed that with the increase of electrode potential in the charge process, R_{SEI} decreases slowly below 3.8 V, decreases rapidly between 3.8 and 3.95 V, and decreases slowly again at more positive potentials, and along with decrease of electrode potential in the discharge process, R_{SEI} increases slowly above 4.0 V, and increases rapidly below 4.0 V. The results demonstrate that the resistance of the SEI film increases and decreases reversibly in the charge-discharge process. There are two possibilities that may lead to the reversible change in R_{SEI}: 1) the resistive SEI film is reversibly breakdown (or dissolution); and 2) the variation in surface electronic conductance of the $LiCoO_2$ cathode is caused by a phase transition of delithiation-lithiation. It can be seen from Figures 7 and 8 that the increase or decrease of R_{SEI} is always concomitant with the increase or decrease of R_e in the charge-discharge process, thus the reversible change of the R_{SEI} in charge-discharge process should be ascribed to the variation in surface electronic conductance of the $LiCoO_2$ cathode.

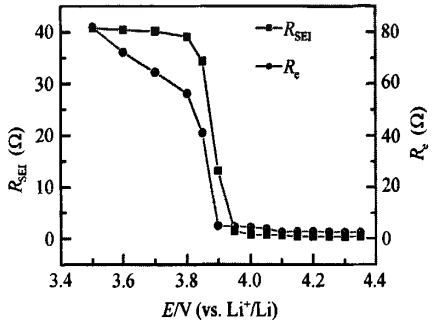

Figure 7 Variations of R_{SEI} and R_e with the increase of the electrode potential obtained from fitting the experimental impedance spectra of the $LiCoO_2$ cathode in the first charge process.

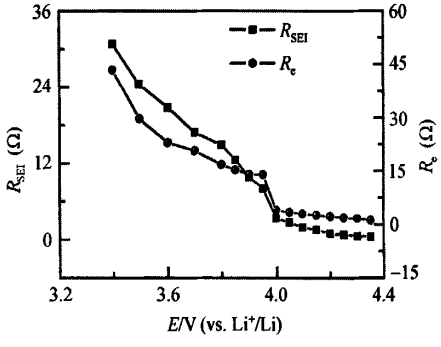

Figure 8 Variations of R_{SEI} and R_e with the decrease of the electrode potential obtained from fitting the experimental impedance spectra of the $LiCoO_2$ cathode in the first discharge process.

When electrode potential is increasing in the charge process, R_e decreases rapidly below 3.9 V, and remains almost invariable above 3.9 V. However, with the decrease of electrode potential in the discharge process, R_e keeps almost invariable above 4.0 V and increases rapidly below 4.0 V. These experimental results are in accordance with those reported by Shibubuya et al.[4], i.e. the electronic conductivity of $LiCoO_2$ increases expo-

nentially with electrode potential in the region from 3.0 to 3.9 V, and the electronic conductivity is saturated above 3.9 V. The potential-conductivity profile shows reasonable reversibility when the potential scan is reversed at 4.0 V. Moreover, R_e is 82 Ω at 3.5 V in the charge process, which is between 2.5 and 5 Ω above 3.9 V, being also in accordance with the results reported by Shibuya et al. that the electronic conductivity of $LiCoO_2$ increases by one or two orders of magnitude.

The above results and discussions demonstrated that assigning the MFA in Nyquist plots of the $LiCoO_2$ cathode to electronic conductive properties of the material could explain the drastic change of the electronic conductivity occurring at the early stage of lithium deintercalation, which has further confirmed our hypothesis and analysis.

2.5 Discussion on the electronic properties of $LiCoO_2$

It is well known that[25–27] $LiCoO_2$ is a p-type semiconductor (band-gap E_g =2.7 eV), while Li_xCoO_2 exhibits a metal-like behavior for $x < 0.75$. Li_xCoO_2 is predicted to have partially filled valence bands for x lower than 1.0. For each Li removed from $LiCoO_2$ lattice, an electron hole is created within the valence band, namely,

$$p = 1 - x, \tag{2}$$

where p is the concentration of electron hole. We may expect that there will be sufficient holes, when x is below 0.75, to allow for a significant degree of screening. And in this regime, the hole state in the valence bands is likely to be delocalized, so that Li_xCoO_2 exhibits metallic-like electronic properties. This behavior is clearly observed in infrared absorption spectra where a strong absorption by holes occurs at low wave-numbers[25]. Accordingly, the variation with potential of electronic conductivity of $LiCoO_2$ in the charge-discharge process may be divided into three regions: 1) the region in which Li_xCoO_2 has a semiconductor-like behavior; 2) the region in which the hole state in the valence bands is likely to be delocalized; 3) the region in which Li_xCoO_2 has a metal-like behavior.

The general expression for the electronic conductivity for p-type semiconductor is given by eq. (3).

$$\sigma = pq\mu, \tag{3}$$

where μ is carrier hole mobility, and q is electron charge.

The electronic resistance R can be written as

$$R = \frac{S}{\sigma l}, \tag{4}$$

where l is the thickness of the material, and S is the material's area.

The Langmuir insertion isotherm could be used for lithium-ion deintercalation from $LiCoO_2$ hosts by assuming that the interaction between the intercalated species and the host material and the interaction between the intercalated species are absent. Thus, the intercalation level, x, is given by[28]

$$x/(1-x) = \exp\left[f(E - E_0)\right], \tag{5}$$

where $f = F/RT$ (F and R, Faraday and gas constant respectively; T, absolute temperature), E and E_0 define the electrode's real and standard potentials in the equilibrium.

When eq. (2) is introduced into eq. (5), the concentration of electron holes is given by

$$p = 1/\left\{1 + \exp\left[f(E - E_0)\right]\right\}. \tag{6}$$

Thus it can be obtained from eqs. (3), (4) and (6):

$$\ln R = \ln(S/q\mu l) + \ln\left\{1 + \exp\left[f(E - E_0)\right]\right\}. \tag{7}$$

When $\exp\left[f(E - E_0)\right]$ is small, as in the present case, $\ln\left\{1 + \exp\left[f(E - E_0)\right]\right\}$ could be linearized by using Taylor series expansion. As a consequence, eq. (7) can be written as

$$\ln R = \ln(2S/q\mu l) + \frac{1}{2} f(E - E_0). \tag{8}$$

It can be seen from Figure 8 that the value of $\ln R$ shows a linear dependence on electrode potential. Therefore, the variation of the electronic conductivity of $LiCoO_2$ in charge-discharge process with potential may be divided into three different parts: 1) when Li_xCoO_2 has a semiconductor-like behavior, the value of $\ln R_e$ shows a linear dependence on electrode potential; 2) when the hole state in the valence bands is likely to be delocalized, the value of $\ln R_e$ increases or decreases drastically with electrode potential; 3) when Li_xCoO_2 has a metal-like behavior, the value of $\ln R_e$ also exhibits a linear dependence on electrode potential.

Figure 9 displays the variations of the logarithm of R_e of $LiCoO_2$ with electrode potential. It can be observed that the experimental values of $\ln R_e$ show a linear dependence on electrode potential below 3.85 V and above 3.9 V, increasing drastically between 3.85 and 3.9 V in

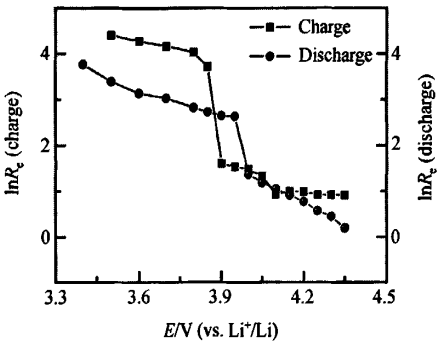

Figure 9 Variations of the logarithm of R_e with the increase and decrease of the electrode potential.

the charge process. However, the linear dependence of the experimental values of $\ln R_e$ on electrode potential is distorted, probably due to the complicated surface phenomena taking place in the first charge process. The experimental values of $\ln R_e$ below 3.95 V and above 4.0 V all show a good linear dependence on electrode potential and the $\ln R_e$ increases drastically between 3.95 and 4.0 V in the discharge process. The above results indicate that the dependence of the experimental values of $\ln R_e$ on electrode potential is in accord with theoretical prediction, which further confirms that the MFA in the Nyquist plots should be attributed to the electronic properties of $LiCoO_2$ caused by delithiation.

3 Conclusions

The storage behavior and the first delithiation-lithiation process of $LiCoO_2$ cathode were investigated by electrochemical impedance spectroscopy. The electronic and ionic transport properties of the $LiCoO_2$ cathode with variation of electrode potential were obtained in 1 $mol \cdot L^{-1}$ $LiPF_6$-EC:DMC:DEC electrolyte solution. It was found that after 9 h storage of the $LiCoO_2$ cathode in the electrolyte solution, a new arc appears in the medium frequency range in Nyquist plots. This new arc increases with increase of the storage time. Moreover, the new arc reversibly increases and decreases with the variation of electrode potential. Such phenomenon corresponds to the variation of electronic conductivity of the $LiCoO_2$ with potential, and the new arc has been ascribed consequently to electronic properties of the $LiCoO_2$ cathode. It has also been revealed that the reversible increase and decrease of the resistance of SEI film in the charge- discharge process might be ascribed to the variation of the surface electronic conductance of the $LiCoO_2$ cathode.

1 Johnson B A, White R E. Characterization commercially available lithium-ion batteries. J Power Sources, 1998, 70: 48−54

2 Antolini E. $LiCoO_2$: formation, structure, lithium and oxygen nonstoichiometry, electrochemical behaviour and transport properties. Solid State Ionics, 2004, 170: 159−171

3 Chen Z, Dahn J R. Methods to obtain excellent capacity retention in $LiCoO_2$ cycled to 4.5 V. Electrochimica Acta, 2004, 49: 1079−1090

4 Shibubuya M, Nishina T, Matsue T, et al. *In situ* conductivity measurements of $LiCoO_2$ film during insertion/extraction by using interdigitated microarray electrodes. J Electrochem Soc, 1996, 143: 3157−3160

5 Tukamoto H, West A R. Electronic conductivity of $LiCoO_2$ and its enhancement by magnesium doping. J Electrochem Soc, 1997, 144: 3164−3168.

6 Lala S M, Montoro L A, Lemos V, et al. The negative and positive structural effects of Ga doping in the electrochemical performance of $LiCoO_2$. Electrochimica Acta, 2005, 51: 7−13

7 Cao H, Xia B, Zhang Y, et al. $LiAlO_2$-coated $LiCoO_2$ as cathode material for lithium ion batteries. Solid State Ionics, 2005, 176: 911−914

8 Ceder G, Van der Ven A. Phase diagrams of lithium transition metal oxides: investigations from first principles. Electrochimica Acta, 1999, 45: 131−150

9 Van der Ven A, Aydinol M K, Ceder G, et al. First-principles investigation of phase stability in Li_xCoO_2. Phys Review B, 1998, 58(6): 2975−2987

10 van Elp J, Wieland J L, Eskes H, et al. Electronic structure of CoO, Li-doped CoO and $LiCoO_2$. Phys Review B, 1991, 44(12): 6090−6103

11 Thomas M G S R, Bruce P G, Goodenough J B. AC impedance analysis of polycrystalline insertion electrodes: Application to $Li_{1-x}CoO_2$. J Electrochem Soc, 1985, 132(7): 1521−1528

12 Gnanaraj J S, Cohen Y S, Levi M D, et al. The effect of pressure on the electroanalytical response of graphite anodes and $LiCoO_2$ cathodes for Li-ion batteries. J Electroanal Chem, 2001, 516: 89−102

13 Levi M D, Gamolsky K, Aurbach D, et al. On electrochemical impedance measurements of $Li_xCo_{0.2}Ni_{0.8}O_2$ and Li_xNiO_2 intercalation electrodes. Electrochimica Acta, 2000, 45: 1781−1789

14 Aurbach D, Markovsky B, Levi M D, et al. New insights into the interactions between electrode materials and electrolyte solutions for advanced nonaqueous batteries. J Power Sources, 1999, 81-82: 95−111

15 Levi M D, Salitra G, Markovsky B, et al. Solid-state electrochemical kinetics of Li-ion intercalation into $Li_{1-x}CoO_2$: simultaneous application of electroanalytical techniques SSCV, PITT, and EIS. J Elec-

trochem Soc, 1999, 146: 1279−1289
16 Nobili F, Dsoke S, Corce F, et al. An ac impedance spectroscopy study of Mg-doped $LiCoO_2$ at different temperatures: electronic and ionic transport properties. Electrochimica Acta, 2005, 50: 2307−2313
17 Nobili F, Tossici R, Croce F, et al. An electrochemical ac impedance study of $Li_xNi_{0.75}Co_{0.25}O_2$ intercalation electrode. J Power Sources, 2001, 94: 238−241
18 Nobili F, Tossici R, Marassi R, et al. An ac impedance study of Li_xCoO_2 at different temperatures. J Phys Chem B, 2002, 106: 3909−3915
19 Croce F, Nobili F, Deptula A, et al. An electrochemical impedance study of the transport properties of $LiNi_{0.75}Co_{0.25}O_2$. Electrochem Commun, 1999, 1: 605−608
20 Nobili F, Croce F, Scrosati B, et al. Electronic and electrochemical properties of $Li_xNi_{1-y}CoO_2$ cathodes studied by impedance spectroscopy. Chem Mater, 2001, 13: 1642−1646
21 Nobili F, Dsoke S, Minicucci M, et al. Correlation of ac-impedance and *in-situ* X-ray spectra of $LiCoO_2$. J Phys Chem B, 2006, 110(23): 11310−11313
22 Wang Z, Huang X, Chen L. Characterization of spontaneous reactions of $LiCoO_2$ with electrolyte solvent for lithium-ion batteries. J Electrochem Soc, 2004, 151: A1641−A1652
23 Wang Z, Chen L. Solvent storage-induced structural degradation of $LiCoO_2$ for lithium ion batteries. J Power Sources, 2005, 146: 254−258
24 Liu N, Li H, Wang Z, et al. Origin of solid electrolyte interphase on nanosized $LiCoO_2$. Electrochem Solid-State Lett, 2006, 9(7): A328−A331
25 Julien C M. Lithium intercalated compounds charge transfer and related properties. Materials Sci Engin R, 2003, 40: 47−102
26 Marianetti C A. Electronic correlations in Li_xCoO_2. Doctor Dissertation. Cambridge: Massachusetts Institute of Technology, 2004. 51−83
27 Van der Ven A. First principles investigation of the thermodynamic and kinetic properties of lithium transition metal oxides. Doctor Dissertation. Cambridge: Massachusetts Institute of Technology, 2000. 46−76
28 Levi M D, Aurbach D. Frumkin intercalation isotherm——A tool for the description of lithium insertion into host materials: a review. Electrochimica Acta, 1999, 45: 167−185

An electrochemical impedance spectroscopic study of the electronic and ionic transport properties of LiCoO2 cathode

作者： ZHUANG QuanChao， XU JinMei， FAN XiaoYong， DONG QuanFeng， JIANG YanXia， HUANG Ling， SUN ShiGang

作者单位： ZHUANG QuanChao(State Key Laboratory of Physical Chemistry of Solid Surfaces, Department of Chemistry, College of Chemistry and Chemical Engineering, Xiamen University, Xiamen 361005, China;Northwest Institute of Nuclear Technology, Xi'an 710024, China)， XU JinMei,FAN XiaoYong,JIANG YanXia,HUANG Ling,SUN ShiGang(State Key Laboratory of Physical Chemistry of Solid Surfaces, Department of Chemistry, College of Chemistry and Chemical Engineering, Xiamen University, Xiamen 361005, China)， DONG QuanFeng(State Key Laboratory of Physical Chemistry of Solid Surfaces, Department of Chemistry, College of Chemistry and Chemical Engineering, Xiamen University, Xiamen 361005, China;Power-long Battery Research Institute, Xiamen University, Xiamen 361005, China)

刊名： 科学通报(英文版) SCI

英文刊名： CHINESE SCIENCE BULLETIN

年，卷(期)： 2007，52(9)

被引用次数： 1次

参考文献(28条)

1. Johnson B A. White R E Characterization commercially available lithium-ion batteries 1998

2. Antolini E LiCoO2:formation,structure,lithium and oxygen nonstoichiometry,electrochemical behaviour and transport properties 2004

3. Chen Z. Dahn J R Methods to obtain excellent capacity retention in LiCoO2 cycled to 4.5 V 2004

4. Shibubuya M. Nishina T. Matsue T In situ conductivity measurements of LiCoO2 film during insertion/extraction by using interdigitated microarray electrodes 1996

5. Tukamoto H. West A R Electronic conductivity of LiCoO2 and its enhancement by magnesium doping 1997

6. Lala S M. Montoro L A. Lemos V The negative and positive structural effects of Ga doping in the electrochemical performance of LiCoO2 2005

7. Cao H. Xia B. Zhang Y LiAlO2-coated LiCoO2 as cathode material for lithium ion batteries 2005

8. Ceder G. Van der Ven A Phase diagrams of lithium transition metal oxides:investigations from first principles 1999

9. Van der Ven A. Aydinol M K. Ceder G First-principles investigation of phase stability in LixCoO2 1998(06)

10. van Elp J. Wieland J L. Eskes H Electronic structure of CoO,Li-doped CoO and LiCoO2 1991(12)

11. Thomas M G S R. Bruce P G. Goodenough J B AC impedance analysis of polycrystalline insertion electrodes:Application to Li1.xCoO2 1985(07)

12. Gnanaraj J S. Cohen Y S. Levi M D The effect of pressure on the electroanalytical response of graphite anodes and LiCoO2 cathodes for Li-ion batteries 2001

13. Levi M D. Gamolsky K. Aurbach D On electrochemical impedance measurements of LixCo0.2Ni0.8O2 and LixNiO2 intercalation electrodes 2000

14. Aurbach D. Markovsky B. Levi M D New insights into the interactions between electrode materials and electrolyte solutions for advanced nonaqueous batteries 1999

15. Levi M D. Salitra G. Markovsky B Solid-state electrochemical kinetics of Li-ion intercalation into Li1-xCoO2:simultaneous application of electroanalytical techniques SSCV,PITT,and EIS 1999

16. Nobili F. Dsoke S. Corce F An ac impedance spectroscopy study of Mg-doped LiCoO2 at different temperatures:electronic and ionic transport properties 2005

17. Nobili F. Tossici R. Croce F An electrochemical ac impedance study of LixNi0.75Coo.2502 intercalation electrode 2001

18. Nobili F. Tossici R. Marassi R An ac impedance study of LixCoO2 at different temperatures 2002

19. Croce F. Nobili F. Deptula A An electrochemical impedance study of the transport properties of LiNi0.75Coo2502 1999

20. Nobili F. Croce F. Scrosati B Electronic and electrochemical properties of LixNi1-yCoO2 cathodes studied by impedance spectroscopy 2001

21. Nobili F. Dsoke S. Minicucci M Correlation of ac-impedance and in-situ X-ray spectra of LiCoO2 2006(23)

22. Wang Z. Huang X. Chen L Characterization of spontaneous reactions of LiCoO2 with electrolyte solvent for lithium-ion batteries 2004

23. Wang Z. Chen L Solvent storage-induced structural degradation of LiCoO2 for lithium ion batteries 2005

24. Liu N. Li H. Wang Z Origin of solid electrolyte interphase on nanosized LiCoO2 2006(07)

25. Julien C M Lithium intercalated compounds charge transfer and related properties 2003

26. Marianetti C A Electronic correlations in LixCoO2 2004

27. Van der Ven A First principles investigation of the thermodynamic and kinetic properties of lithium transition metal oxides 2000

28. Levi M D. Aurbach D Frumkin intercalation isotherm-A tool for the description of lithium insertion into host materials:a review 1999

相似文献(10条)

1. 期刊论文 LI Jinhui. ZHONG Shengwen. XIONG Daoling. CHEN Hao Synthesis and electrochemical performances of LiCoO2 recycled from the incisors bound of Li-ion batteries -稀有金属（英文版） 2009,28(4)

A new LiCoO2 recovery technology for Li-ion batteries was studied in this paper. LiCoO2 was peeled from the Al foil with dimethyl acetamide (DMAC), and then polyvinylidene fluoride (PVDF) and carbon powders in the active material were eliminated by high tempera- 1.00. The new LiCoO2 was obtained by calcining the mixture at 850℃ for 12 h in air. The structure and morphology of the recycled powders and resulting samples were studied by XRD and SEM techniques, respectively. The layered structure of LiCoO2 synthesized by adding Li2CO3 is the best, and it is found to have the best characteristics as a cathode material in terms of charge-discharge capacity and cycling mAh.g-1.

2. 期刊论文 ZHUANG QuanChao. XU JinMei. FAN XiaoYong. WEI GuoZhen. DONG QuanFeng. JIANG YanXia. HUANG Ling. SUN Shigang LiCoO2 electrode/electrolyte interface of Li-ion batteries investigated by electrochemical impedance spectroscopy -中国科学B辑（英文版） 2007,50(6)

The storage behavior and the first delithiation of LiCoO2 electrode in 1 mol/L LiPF6-EC:DMC:DEC electrolyte were investigated by electrochemical impedance spectroscopy (EIS). It has found that, along with the increase of storage time, the thickness of SEI film increases, and some organic carbonate lithium compounds are formed due to spontaneous reactions occurring between the LiCoO2 electrode and the electrolyte. When electrode potential is changed from 3.8 to 3.95 V, the reversible breakdown of the resistive SEI film occurs, which is attributed to the reversible dissolution of the SEI film component. With the increase of electrode potential, the thickness of SEI film increases rapidly above 4.2 V, due to overcharge reactions. The inductive loop observed in impedance spectra of the LiCoO2 electrode in Li/LiCoO2 cells is attributed to the formation of a Li1-xCoO2/LiCoO2 concentration cell. Moreover, it has been demonstrated that the lithium-ion insertion-deinsertion in LiCoO2 hosts can be well described by both Langmuir and

Frumkin insertion isotherms, and the symmetry factor of charge transfer has been evaluated at 0.5.

3.外文期刊 ZHUANG QuanChao.XU JinMei.FAN XiaoYong LiCoO2 electrode/electrolyte interface of Li-ion batteries investigated by electrochemical impedance spectroscopy

The storage behavior and the first delithiation of LiCoO2 electrode in 1 mol/L LiPF6-EC:DMC:DEC electrolyte were investigated by electrochemical impedance spectroscopy(EIS).It has found that,along with the increase of storage time,the thickness of SEI film increases,and some organic carbonate lithium compounds are formed due to spontaneous reactions occurring between the LiCoO2 electrode and the electrolyte.When electrode potential is changed from 3.8 to 3.95 V,the reversible breakdown of the resistive SEI film occurs,which is attributed to the reversible dissolution of the SEI film component.With the increase of electrode potential,the thickness of SEI film increases rapidly above 4.2 V,due to overcharge reactions.The inductive loop observed in impedance spectra of the LiCoO2 electrode in Li/LiCoO2 cells is attributed to the formation of a Li_(1-x)CoO2/LiCoO2 concentration cell.Moreover,it has been demonstrated that the lithium-ion insertion-deinsertion in LiCoO2 hosts can be well described by both Langmuir and Frumkin insertion isotherms,and the symmetry factor of charge transfer has been evaluated at 0.5.

4.期刊论文 姚晓林.张承平.陈春华.YAO Xiao-lin.ZHANG Cheng-pin.CHEN Chun-hua LiNixMn2-xO4对锂离子电池材料LiCoO2的表面改性研究 -中国科学技术大学学报2009,39(4)

在锂离子电池正极材料LiCoO2表面上修饰LiNixMn2-xO4来改善LiCoO2在循环过程中的容量衰减问题.对所得产物进行了XRD、SEM表征,并进行了充放电容量测试和交流阻抗测试.通过XRD和SEM,发现LiNixMn2-xO4修饰没有改变材料的晶体结构.在电化学性能测试中,由于包覆LiNixMn2-xO4可以减少材料与电解液的直接接触,最大程度地减缓电极材料在电化学循环时结构遭到破坏,在修饰量较小(3 5%)时,该改性方法改善了LiCoO2电极的循环性能,69次循环后放电比容量没有衰减,且大大地提高了平台效率.

5.外文期刊 Tournadre. F.Croguennec. L.Willmann. P.Delmas. C On the mechanism of the P2-Na0.70CoO2 -> O2-LiCoO2 exchange reaction - Part II: an in situ X-ray diffraction study

A model was proposed to describe the exchange reaction of sodium by lithium in P2 crystals, it was based first on the formation of nucleation centers and then on the growth of O2 domains in P2 crystals from these nucleation centers. This study has shown that depending on the ratio between the growing and nucleation speeds, O2, O6 or faulted structures are obtained and that this model allows a good analysis of the exchange process. XRD patterns simulation and their comparison with that of experimental O2-LiCoO2 have shown that there was almost no defects in the O2-LiCoO2 structure obtained by ion exchange in water. Therefore, this study has shown that the growth of the O2 domains in the P2-Na0.7CoO2 crystals is faster than the formation of nucleation centers.This P2-Na0.7CoO2-->O2-LiCoO2 exchange reaction was also studied in situ by X-ray diffraction; simulations of key XRD patterns by P2-O2 intergrowths were also achieved. It was shown, in good agreement with the simulations, that the growth of O2 domains was faster than the formation of the nucleation centers and kinetically activated by a P2-Na0.70CoO2 --> P2* - Nasimilar toO.50CoO2 phase transition. For those reasons, the P2-Na0.70CoO2 --> O2-LiCoO2 exchange reaction in water leads to an O2 phase, with an almost ideal packing. (C) 2004 Elsevier Inc. All rights reserved.

6.期刊论文 刘云建.胡启阳.李新海.王志兴.郭华军.彭文杰.LIU Yun-jian.HU Qi-yang.LI Xin-hai.WANG Zhi-xing.GUO Hua-jun.PENG Wen-jie 锂离子电池边角料中直接回收合成LiCoO2的性能 -中国有色金属学报2008,18(z1)

研究了一种从锂离子蓄电池正极片的边角料中直接回收钴酸锂的新工艺.先用二甲基乙酰胺(DMAC)浸泡正极片,将LiCoO2从铝箔上剥离,再在高温下除去正极中的聚偏氟乙烯(PVDF)和碳粉等杂质.然后添加不同的锂盐(Li2CO3、LiOH·H2O和 LiAc·2H2O)调节回收粉末中的Li与Co的量比为1.00,再在850℃下焙烧12 h得到最终产品.用扫描电子显微镜(SEM)和X射线衍射(XRD)分析技术对得到的样品进行微观形貌与晶相结构的研究.研究结果表明,添加Li2CO3合成的LiCoO2层状结构发育最为完善,其首次放电容量和循环性能也最好;在3.0~4.3 V进行充放电,首次放电容量达到160 mA·h/g,经30次循环以后,仍有150 mA·h/g.

7.期刊论文 汤宏伟.徐秋红.常照荣.李云平.齐霞.TANG Hong-wei.XU Qiu-hong.CHANG Zhao-rong.LI Yun-ping.Qi Xia 锂离子电池正极材料LiCoO2的制备 -电池2005,35(2)

将前驱体CoOOH(通过自制的连续式反应器,采用湿法合成制备)和LiOH·H2O,通过固相反应法合成了结晶度好的LiCoo2.差热-热重分析表明:650℃就已经反应完全;X射线衍射结果表明:合成的材料具有完美的层状结构;扫描电镜显示:CoOOH在焙烧过程中,边缘开始球化;IR分析说明:LiCoO2中Co-O吸收峰向低波数方向偏移.

8.外文期刊 Ni. C. T..Fung. K. Z. Effect of chitosan on deposition of LiCoO2 thin film for Li-ion batteries

Deposition of LiCoO2 thin film using chitosan-added precursor solution was found to be a cost-effective way to fabricate cathode for Li-ion thin film batteries. The structures and electrochemical performance of such LiCoO2 cathode were characterized by using an X-ray diffracotmeter (XRD), FTIR and charge-discharge tests. After annealing at ca. 500 degrees C, the results of XRD showed that the LiCoO2 gel started to crystallize and showed hexagonal phase with a space group of Rim. The enhanced stability of the precursor solution by the addition of chitosan is attributed to the complexation between metal ions and the -NH2 groups of chitosan. The electrochemical behaviour for the deposited films calcined at 700 degrees C for 4 h was also characterized by charge-discharge test. The result revealed that the film deposited from chitosan-containing precursor solution possesses an initial discharge capacity of 129 mAh g(-1).

9.期刊论文 武雪峰.王振波.张明艳.WU Xue-feng.WANG Zhen-bo.ZHANG Ming-yan LiMn2O4/LiCoO2共混对锂离子电池性能的影响 -电池工业2010,15(2)

将LiMn2O4和LiCoO2在强力混合机中混合均匀,获得均匀的共混正极材料.通过电化学测试研究了LiMn2O4/LiCoO2两种电极材料混合比例对锂离子电池循环性能的影响,并比较了LiMn2O4与LiCoO2混合前后在常温和高温环境下循环性能的差异.实验结果表明:在LiMn2O4与LiCoO2共混后制得的锂离子电池在常温和高温环境下都具有良好的循环性能.

10.期刊论文 LIU Yun-jian.HU Qi-yang.LI Xin-hai.WANG Zhi-xing.GUO Hua-jun Recycle and synthesis of LiCoO2 from incisors bound of Li-ion batteries -中国有色金属学会会刊（英文版） 2006,16(4)

A new LiCoO2 recovery technology of Li-ion battery was studied. LiCoO2 was initially separated from the Al foil with dimethyl acetamide(DMAC), and then the polyvinylidene fluoride(PVDF) and carbon powders in the active material were eliminated by high

temperature calcining. The content of the elements in the recovered powder was analyzed. The structure and morphology of the resulted samples were observed by XRD and SEM. Then the Li2CO3 was added in the recycled powder to adjust the Li/Co molar ratio to 1. The new LiCoO2 was synthesized by calcining at 850 ℃ for 12 h in air. The well-crystallized single phase LiCoO2 without Co3O4 phase was obtained. The recycle-synthesized LiCoO2 powders have good characteristics as a cathode active material in terms of charge-discharge capacity and cycling performance.

引证文献(1条)

1.ZHUANG QuanChao.TIAN LeiLei.WEI GuoZhen.DONG QuanFeng.SUN ShiGang Two-and three-electrode impedance spectroscopic studies of graphite electrode in the first lithiation[期刊论文]-科学通报（英文版） 2009(15)